RESEARCH

Synthesis and biological activities of 3-aminoimidazo[1,2-α]pyridine compounds

Isra Al-Qadi[1], Michel Hanania[2], Ismail Warad[1], Nisreen Al-Hajj[1], Rand Hazzam[1], Yousef Salama[3], Saki Raheem[4*] and Nawaf Al-Maharik[1*]

Abstract Despite their importance in cancer treatment, anticancer compounds face significant challenges due to drug resistance and low specificity, creating an urgent need for the discovery of more effective alternative. Herein, we report the synthesis of eleven 3-aminoimidazole[1,2-α]pyridine compounds (9–19) employing the one-pot Groebke-Blackburn-Bienayme three-component reaction (GBB-3CR). The cytotoxicity of the synthesised compounds was evaluated against three cancer cell lines (MCF-7, HT-29, B16F10) and a normal cell (MEF). Considering effectiveness and safety, the results demonstrated that among the eleven synthesised compounds, only compounds 12 and 14 exhibited high inhibitory activity against cancer cell lines. Compound 12 with a nitro group at the C-2 position and a *p*-chlorophenyl group at C-3 position, showed the highest inhibitory activity against HT-29, with an IC_{50} of 4.15 ± 2.93 µM. Additionally, compound 14, with a tolyl moiety at the C-2 position and a *p*-chlorophenyl amine at C-3 position, can also be considered a promising bioactive product against B16F10, with an IC_{50} of 21.75 ± 0.81 µM. Further research on these compounds may yield more potent candidates for the development of new anticancer agents.

Keywords Anticancer, 3-aminoimidazole[1,2-α]pyridine, 4-chlorophenyl isonitrile, GBB-3CR, Multicomponent reaction

Introduction

Bioactive organic molecules often contain nitrogen-based heterocycles, which exhibit a broad spectrum of biological activities [1–10]. Imidazole[1,2-α]pyridines **1** play a crucial role as key structural constituents in

*Correspondence:
Saki Raheem
s.raheem@westminster.ac.uk
Nawaf Al-Maharik
n.maharik@najah.edu
[1] Department of Chemistry, Faculty of Science, An-Najah National University, Nablus 00970, Palestine
[2] Department of Chemistry, Faculty of Applied Sciences, Technology and Engineering, Bethlehem University, Bethlehem 00970, Palestine
[3] Department of Biomedical Sciences, Faculty of Medicine and Health Sciences, An-Najah National University, Nablus 00970, Palestine
[4] School of Life Sciences, University of Westminster, 115 New Cavendish Street, London W1W 6UW, UK

several compounds. Recently, researchers have discovered that imidazole[1,2-α]pyridine scaffolds exhibit remarkable biological characteristics, serving various purposes such as antiviral [4, 11], antiprotozoal [12], anticancer [1–9, 13], and antimicrobial [14] activities. The various biological effects of these compounds have prompted continuous efforts to accelerate the development of novel synthetic methods for producing derivatives with structural variations at the 2- and 3- positions of the moiety. The synthetic methods encompass a range of techniques, including condensation reactions, oxidative coupling, one-pot multicomponent procedures, hydroamination reactions, and amino-oxygenation reactions [15]. The Groebke-Blackburn-Bienayme three-component reaction (GBB-3CR) is an efficient and cost-effective method for synthesizing imidazole[1,2-α]pyridines [16–18] offering the ability to modify the structure in three

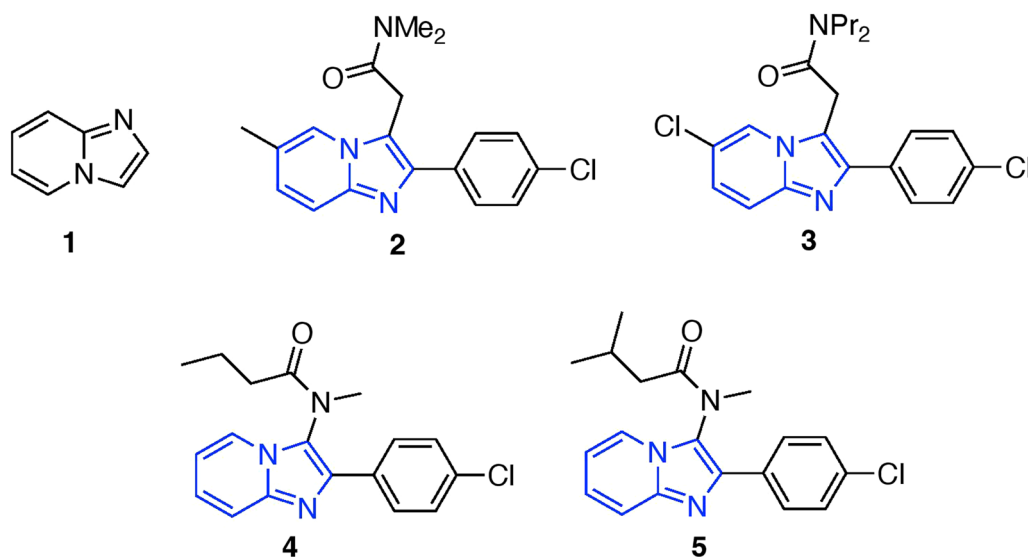Al-Qadi *et al. BMC Chemistry*   (2025) 19:48

Page 2 of 15

Fig. 1 Chemical structure of imidazopyridine and derivatives featuring the imidazopyridine scaffold

or more regions. The GBB-3CR has led to the development of various medicines and lead compounds, including zolpidem **2**, alpidem **3**, saripidem **4**, and necopidem **5** (Fig. 1). The GBB reaction involves one-pot acid-catalyzed condensation of aminoazines with aldehyde and isocyanides. Although there have been notable advancements in drug therapies over the last ten years, cancer remains a substantial health obstacle. Cancer treatment now includes advanced modalities beyond conventional methods. Natural product therapy uses bioactive compounds from plants to target cancer pathways with fewer side effects [19]. Exosome-base therapy utilizes exosomes for precise drug delivery to cancer cells [20]. Stem cell therapy offers potential in regenerating damages tissues or delivering targeted treatments to resistant tumors [21]. Gene therapy modifies faulty gene or actives the immune system to combat cancer [22]. Nanoparticle-based therapy enhances drug delivery and imaging, targeting cancer cells precisely while sparing healthy tissues [23, 24]. Additionally, radiation therapy and immunotherapy remain crucial, using high-energy radiation and boosting the immune system to effectively treat various cancers [25, 26]. These innovative approaches are revolutionizing cancer treatment with more effective and personalized options.

This study aims to synthesize imidazo[1,2-α]pyridine derivatives (Fig. 2) utilizing GBB-3CR and to assess their potential as anticancer agents. The structural determination of the novel compounds was accomplished using ^{1}H- and ^{13}C-NMR, IR, and XDR-single techniques.

Results and discussion
Synthesis
The imidazo[1,2-α]pyridine derivatives were produced using acid-catalyzed GBB-3CR, as illustrated in Fig. 3. The procedure involved the condensation of 2-amino-pyridine **6** with various aldehydes **7a-k**, employing a small quantity of *p*-toluenesulfonic acid or scandium triflate as catalysts [18]. This was followed by cyclization of the resulting imide intermediate with 4-chlorophenyl isocyanide **8**. The presence of electron-donating (ED) groups on the benzaldehydes, such as the methoxy group in **15**, the methyl group in **14** and the benzene rings in **16**, may result in moderate yields, higher than the yield obtained for compound **19**, which bears the electron-withdrawing (EW) trifluoromethyl (CF_3) group (Fig. 2). The product's moderate yield (30–50%) could be ascribed to the utilization of repeated flash chromatography and recrystallization to obtain the very pure compounds required for biological screening. The compounds' purity was evaluated by HPLC, HRLM and elemental analysis. Additionally, the structure of the key pharmacophore, imidazo[1,2-α]pyridine, was validated using single-crystal X-ray crystallography on compound **15**.

X-Ray and DFT analysis
Figure 4 shows the X-ray diffraction (XRD) and density functional theory (DFT) analyses conducted to verify the three-dimensional arrangement of compound **15**. This compound was used as a reference because all the compounds synthesised in this study feature three aromatic rings with an imidazole[1,2-α]pyridine unit. Table S1 and Fig. 4a depict the XRD-ORTEP, while Fig. 4b highlights
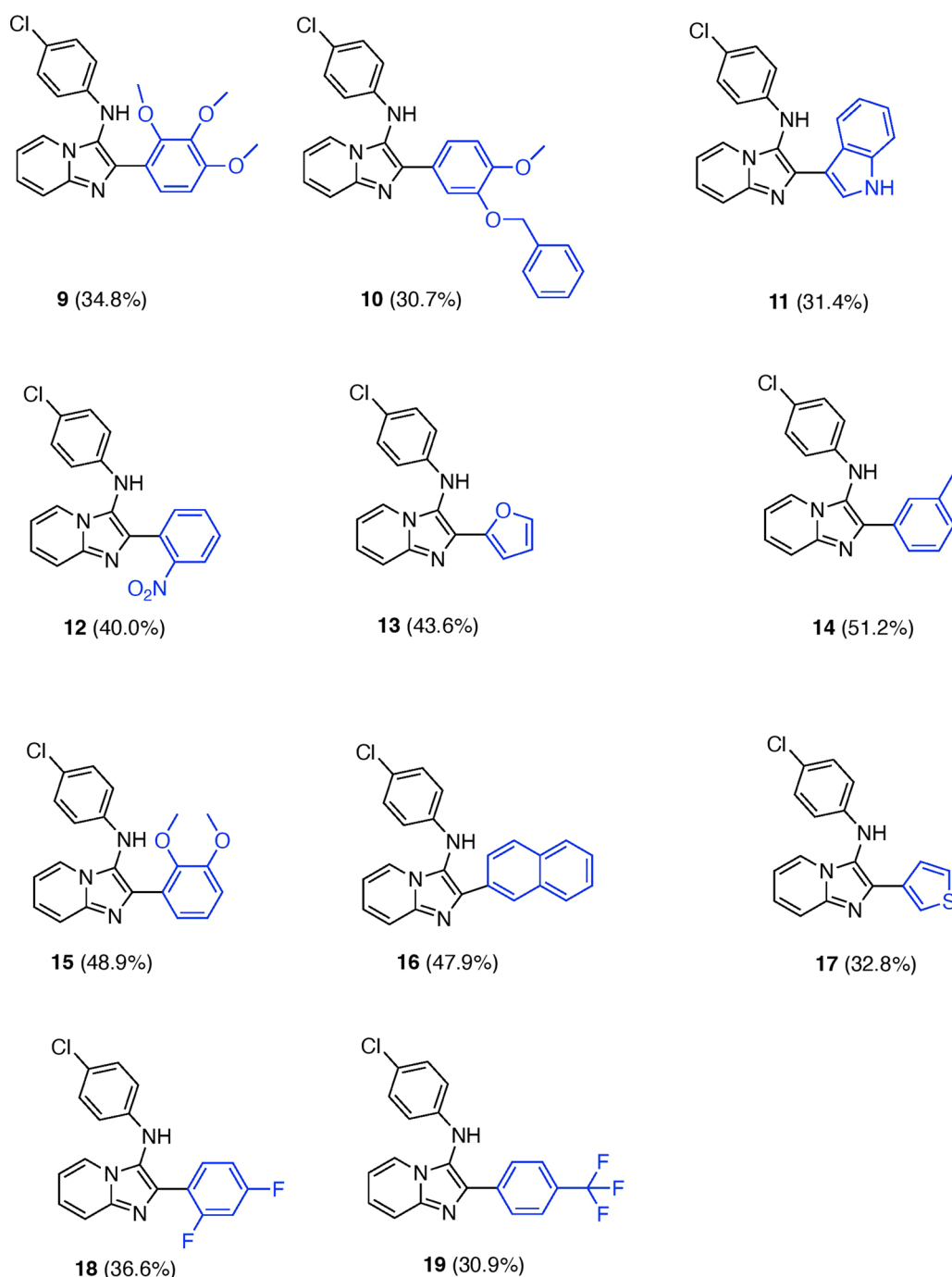
Al-Qadi *et al. BMC Chemistry*   (2025) 19:48

Page 3 of 15

Fig. 2 Structure–activity relationships of the synthesized compounds 9–19

the DFT-optimized molecular structure. Compound **15** was crystallized in an orthorhombic crystal system with the $P2_12_12_1$ space group. The crystal structure obtained has the following lattice parameters: a = 10.2676 Å, b = 11.1678 Å, and c = 16.8317 Å. X-ray measurements showed the presence of three aromatic rings with the imidazo[1,2-α]pyridine unit in a semi-perpendicular

shape to each other, forming a fun wing-like structure. The formation of the *N*-phenylimidazo unit has also been confirmed, as the N-H unit was identified by SC-XRD, as shown in Fig. 4a. A densely orthorhombic molecular packing structure with a Z-factor of 4 has been observed in the crystal lattice of the desired molecule (Fig. 4b). The DFT optimization structure (Fig. 4c) confirmed the
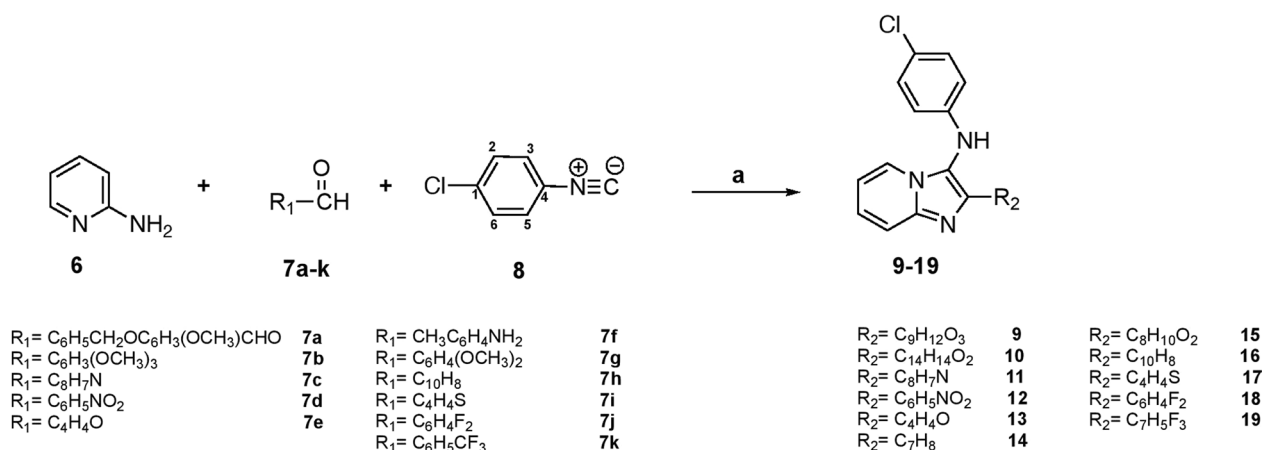
Al-Qadi *et al. BMC Chemistry*   (2025) 19:48

Page 4 of 15

Fig. 3 Reagents and conditions: **a** p -TsA.H 2 O or Sc(OTf) 3 , MeOH: CH 2 Cl 2 (1:1) or MeOH only., 1 h, 50 °C
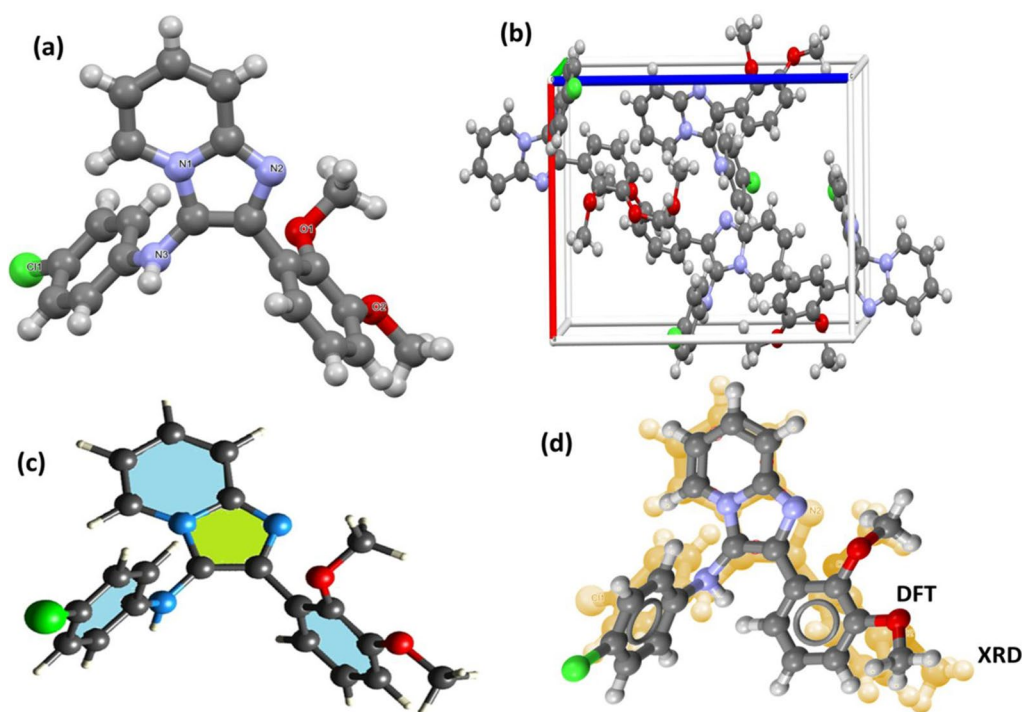

Fig. 4 a 3D-XRD, **b** B3LYP/molecular struccture, **c** DFT/XDR structure matching and **d** crystal packing module

SC-XRD collections regarding the 3-D structure, atom orientation, and structural parameters like angles, torsions, and bond lengths, as seen in Fig. 4d and Table S1.

XDR/HSA-Interactions

The synthesized compound **15** had a molecular structure that was defined by the formation of many non-classical and classical H-bond interactions, such as C-H...O/C-H...Cl and N-H...N. These interactions lead to the creation of two main types of new 2D-synthons without 1D-chain interactions. The molecular structure of the desired ligand is distinguished by the accumulation of classical N-H...N H-bond and C-H...C=N interactions with 2.021 and 2.850 Å bond lengths, respectively, constructing two 2D-S10 synthons per molecule (Fig. 5a). The second synthon was S13 (2 per molecule), formed by combining C-H...O and C-H...πPh interactions with 2.617 and 2.878 Å bond lengths, respectively (Fig. 5b).
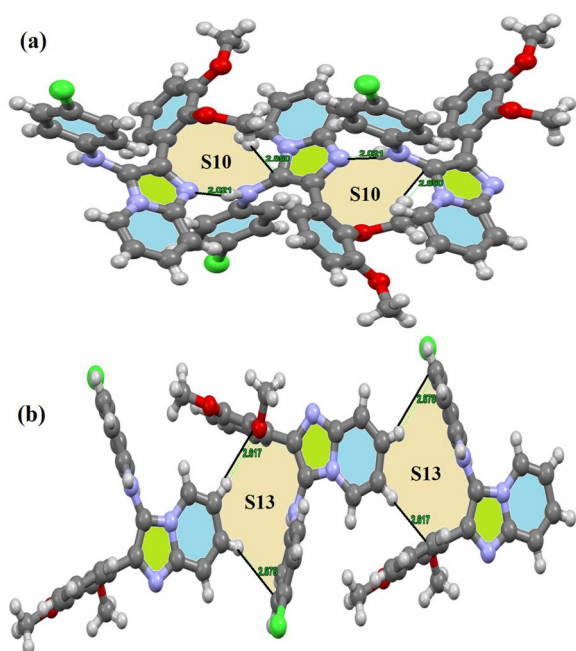
Al-Qadi *et al. BMC Chemistry*   (2025) 19:48

Page 5 of 15

Fig. 5 **a** S10, and **b** S13 synthons formed in the X-ligand lattice

Figure 6 presents the HSA analysis, which provides vital information about the intermolecular interactions taking place within the computed molecule and its surroundings. The HSA analysis utilizes a color-mapped representation that ranges from − 0.462 (shown as blue) to 1.567 (represented as red). The dnorm surface (Fig. 6a) displays five prominent red areas, indicating the type and strength of interactions per molecule. Moreover, the dnorm surface shows significant interactions, such as two classical short N–H...N H-bond interactions per molecule and several non-classical C–H...O H-bond interactions. Furthermore, the dnorm surface exhibits the major interactions required, including the classical presence of two short N–H...N hydrogen bond interactions per molecule, as well as multiple non-classical C–H...O hydrogen bond interactions.

The shape index (Fig. 6b) indicated the presence of electron concentrations surrounding functional groups such as C–O, C–Cl, and C–N, which were visually represented by surfaces in red, blue, and orange. The presence of blue surrounding surface atoms, particularly hydrogen atoms, along with the red color representing O, N, Cl, and other highly electronegative atoms (Fig. 6c), promotes the formation of polarized bonds, such as hydrogen bonds. In addition, the 2D-FP computations depicted in Fig. 6c, verified the presence of intermolecular contacts and determined the proportion of atom-to-atom interactions (H···.X%) in the following order: H....H(46.9%) > C....H(11.3%) > Cl....H(4%) > O....H (2.8%) > N....H(2.6%). The contributions of the H-atoms were found to be greater than those of the C-atoms, which were in turn greater than those of the Cl-atoms (Fig. 6c); this was confirmed by practical XRD observations in the crystal lattice.
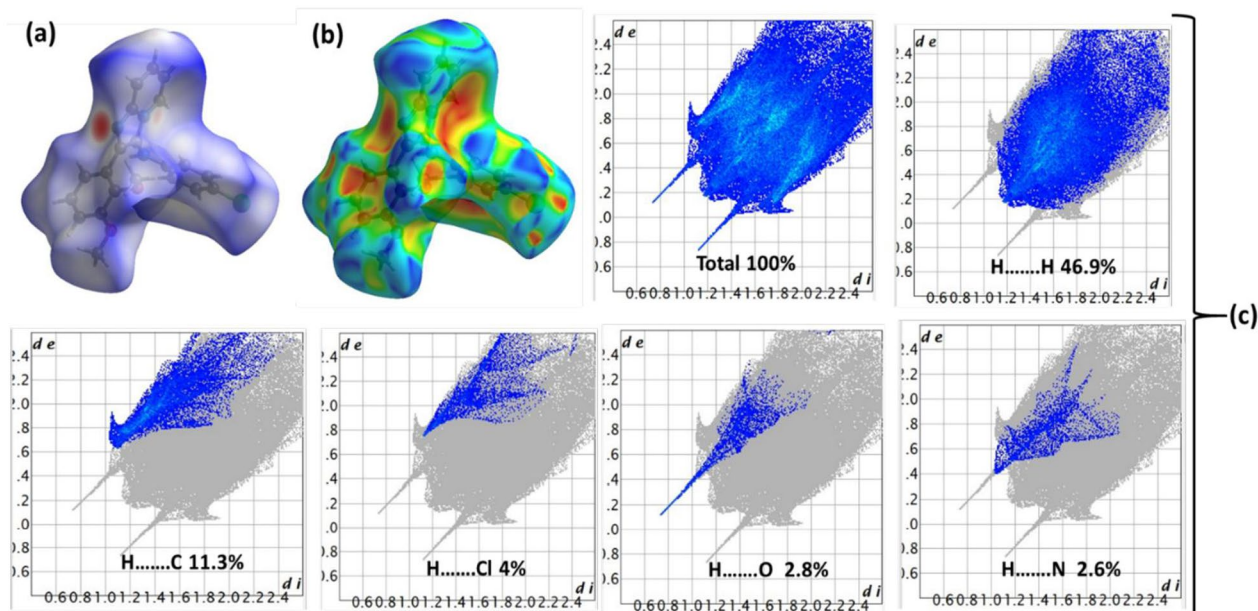

Fig. 6 **a** dnorm **b** shape-index, and **c** 2D-FP atom-to-atom ration

Al-Qadi *et al. BMC Chemistry*   (2025) 19:48

Page 6 of 15

Biological activity

Anticancer activity

The cytotoxicity of the synthesized imidazo[1,2-*a*]pyridine compounds (9–19) were screened against breast (MCF-7), colon (HT-29) and melanoma (B16F10) cancer cell lines, as well as normal cell line (MEF) as shown in Table 1.

Cytotoxic analysis of synthesized compounds revealed that imidazopyridine compound 18 showed the highest cytotoxicity against MCF-7 with $IC_{50} = 14.81 \pm 0.20$ μM, followed by compound 11, which has an indole moiety at the C-2 position, with $IC_{50} = 20.47 \pm 0.10$ μM. However, compound 12 with an EW group (nitro) is effective against MCF-7 with $IC_{50} = 30.88 \pm 14.44$ μM and had moderate cytotoxicity against B16F10 ($IC_{50} = 64.81 \pm 15.78$ μM). Compound 13, bearing a furan moiety at the C-2 position, showed weak bioactivity against B16F10 ($IC_{50} = 197.06 \pm 14.42$ μM) and moderate anticancer activity against MCF-7 ($IC_{50} = 66.48 \pm 37.87$ μM). On the other hand, compounds 9, 10, 15 and 17 were ineffective against MCF-7 as well as the other two cell lines.

The imidazopyridine compound 12, with a nitro group on the moiety substituted at the C-2 position and a *p*-chlorophenyl ring at the C-3 position, demonstrated the highest inhibitory activity against HT-29 cell, with an IC_{50} value of 4.15 ± 2.93 μM. The next highest level of cytotoxicity against this cancer cell line was exhibited by compound 18, with an IC_{50} value of 10.11 ± 0.70 μM. Additionally, compound 11 also showed high anticancer activity against this cancer cell line with IC_{50} value of 18.34 ± 1.22 μM. This value was similar to the high activity of this compound against MCF-7, in contrast to its moderate cytotoxicity against B16F10 ($IC_{50} = 39.20 \pm 1.84$ μM). Compounds 13 and 14 also exhibited moderate inhibitory activity against HT-29, with IC_{50} values of 48.31 ± 0.53 and 44.45 ± 0.15 μM, respectively.

The imidazopyridine compound 18, with a 2,4 difluorophenyl moiety substituted at the C-2 position and a *p*-chlorophenyl amine at the C-3 position, displayed the highest inhibitory activity against B16F10 with an IC_{50} of 14.39 ± 0.04 μM. Compound 14, which had a tolyl moiety at the C-2 position and *p*-chlorophenyl amine at the C-3 position, showed the next highest cytotoxicity value, with an IC_{50} of 21.75 ± 0.81 μM. However, compound 16, which contains a naphthalene moiety at the C-2 position, exhibited good anticancer activity, with an IC_{50} values of 84.05 ± 3.37 and 93.08 ± 0.61 μM against MCF-7 and HT-29, respectively, while it was inactive against B16F10. Additionally, compound 19, which had an EW group (trifluoromethyl) at the C-2 position, was ineffective against MCF-7 and B16F10 ($IC_{50} \geq 200$ μM); however, it showed good inhibitory activity against HT-29 with an IC_{50} of 85.50 ± 18.83 μM.

Therefore, this study conducted a further assessment of the cytotoxic effects of the synthesized compounds on the normal cell line MEF. Among the promising bioactive compounds, compound 11 was the most cytotoxic against normal cells ($IC_{50} = 1.84 \pm 0.83$ μM), followed by compounds 18 ($IC_{50} = 16.31 \pm 0.08$ μM) and 13 ($IC_{50} = 32.93 \pm 0.09$ μM). Other bioactive compounds that showed moderate cytotoxicity against MEF include compound 12 ($IC_{50} = 40.54 \pm 4.34$ μM) and compound 19 ($IC_{50} = 63.85 \pm 2.33$ μM). As previously described, compound 11 showed high toxicity against MCF-7 and HT-29 ($IC_{50} < 20.47$ μM), but it was also very toxic against normal cells ($IC_{50} < 1.84$ μM). Additionally, compound 13 showed cytotoxicity against normal cells with an IC_{50} of 32.93 ± 0.09 μM, which is lower than the IC_{50} reported against cancer cell lines ($IC_{50} > 45.00$ μM). Although compound 18 was potent against the three cancer cell lines ($IC_{50} < 15.00$ μM), it was also cytotoxic against MEF, with a value approximately similar ($IC_{50} = 16.31 \pm 0.08$ μM). For these reasons, the bioactivity of compounds 11, 13, and 18 was not considered at this stage. Compound 12 is a more potent against HT-29, with an IC_{50} of 4.15 ± 2.93 μM, while its cytotoxicity against normal cells is tenfold lower ($IC_{50} = 40.54 \pm 4.34$ μM). For the same reasons, compound 14 can be considered a promising bioactive product against B16F10, with an IC_{50} of 21.75 ± 0.81 μM versus >200 μM against MEF. These IC_{50} values demonstrate the high selectivity of the two promising compounds 12 and 14, against cancer cells compared to normal cells, as confirmed by the histograms in Fig. 7.

In comparison to the control (untreated cancer cells), the three cancer cell lines (MCF-7, HT-29, and B16F10) were investigated for morphological changes after being treated with the synthesized compounds 9–19. As shown in Fig. 8, cells of the HT-29 and B16F10 cell lines showed shrinkage and lost their original form when treated with compounds 12 and 14 at high concentrations (≥ 50 μg/ml).

Conclusions

The present study describes the synthesis of imidazo[1,2-a]pyridine compounds (9–19) utilizing an acid-catalyzed GBB-3CR. All synthesized compounds were screened for cytotoxic activity against the cancer cell lines MCF-7, HT-29, and B16F10, as well as the normal MEF cell line, using the Trypan Blue Exclusion Assay. Analysis of the synthesized compounds, based on their efficacy and safety, indicated that imidazopyridines 12 and 14, with para-chlorophenyl at C-3, and nitro and methyl groups substituted on the phenyl ring at C-2, respectively, were

Table 1 In vitro antiproliferative activity data of compounds 9–19
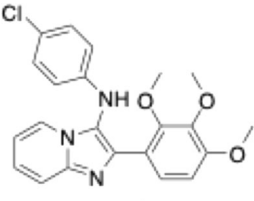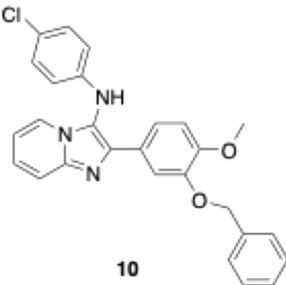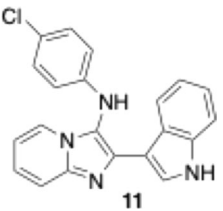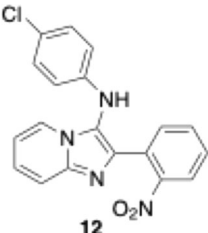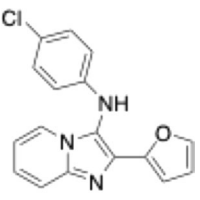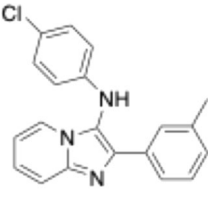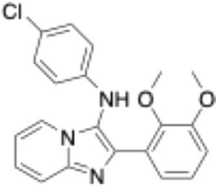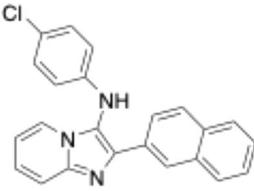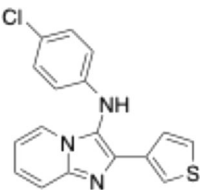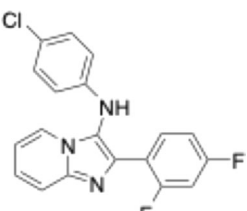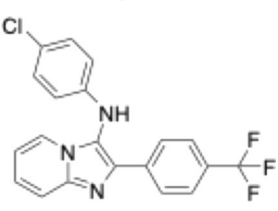
Cpd's designation	[a]IC$_{50}$ (μM)			
	MCF-7	HT-29	B16F10	MEF
Paclitaxel (Taxol)	0.00834	0.0166	55.7	17.23
9	> 200	> 200	> 200	> 200
10	> 200	> 200	> 200	18.5 ± 0.33
11	20.47 ± 0.10	18.34 ± 1.22	39.2 ± 1.84	1.84 ± 0.83
12	30.88 ± 14.44	4.15 ± 2.93	64.81 ± 15.78	40.54 ± 4.34
13	66.48 ± 37.87	48.31 ± 0.53	197.06 ± 14.42	32.93 ± 0.09
14	195.26 ± 19.89	44.45 ± 0.15	21.75 ± 0.81	> 200

Al-Qadi *et al. BMC Chemistry*   (2025) 19:48

Page 8 of 15

Table 1 (continued)

Cpd's designation	$^{a}IC_{50}$ (µM)			
	MCF-7	HT-29	B16F10	MEF
15	> 200	> 200	> 200	> 200
16	84.05 ± 3.37	93.08 ± 0.61	> 200	> 200
17	> 200	> 200	> 200	> 200
18	14.81 + 0.20	10.11 ± 0.70	14.39 ± 0.04	16.31 ± 0.08
19	> 200	85.50 ± 18.83	195.45 ± 15.30	63.85 ± 2.33

[a] The IC_{50} values (µM) represent an average of two independent experiments (mean ± SD)

potent anticancer agents against the HT-29 (colon) and B16F10 (melanoma) cancer cell lines (Fig. 8).

While this study synthesized eleven imidazo[1,2-a] analogues with variations exclusively in the aldehyde component, the choice of p-chlorophenyl isonitrile was primarily due to its known reactivity and effectiveness in facilitating the desired reaction under specified conditions. Additionally, it provided a consistent structural framework for assessing the impact of aldehyde variations on the biological activity of the resulting compounds. One constraint of this study was the focus on a single isocyanide, which limited the diversity of structural analogues. Future studies will aim to explore a broader range of isocyanides and various 2-aminoazines to evaluate their influence on reaction scope and the biological properties of the synthesized analogues.

Fig. 7 Quantitative analysis of invasive cell number

Fig. 8 Morphological changes of the most potent synthesized compounds treated with cancer and normal cell lines and controls (untreated cancer cells)

Al-Qadi *et al. BMC Chemistry* (2025) 19:48

Page 10 of 15

Experimental

General information

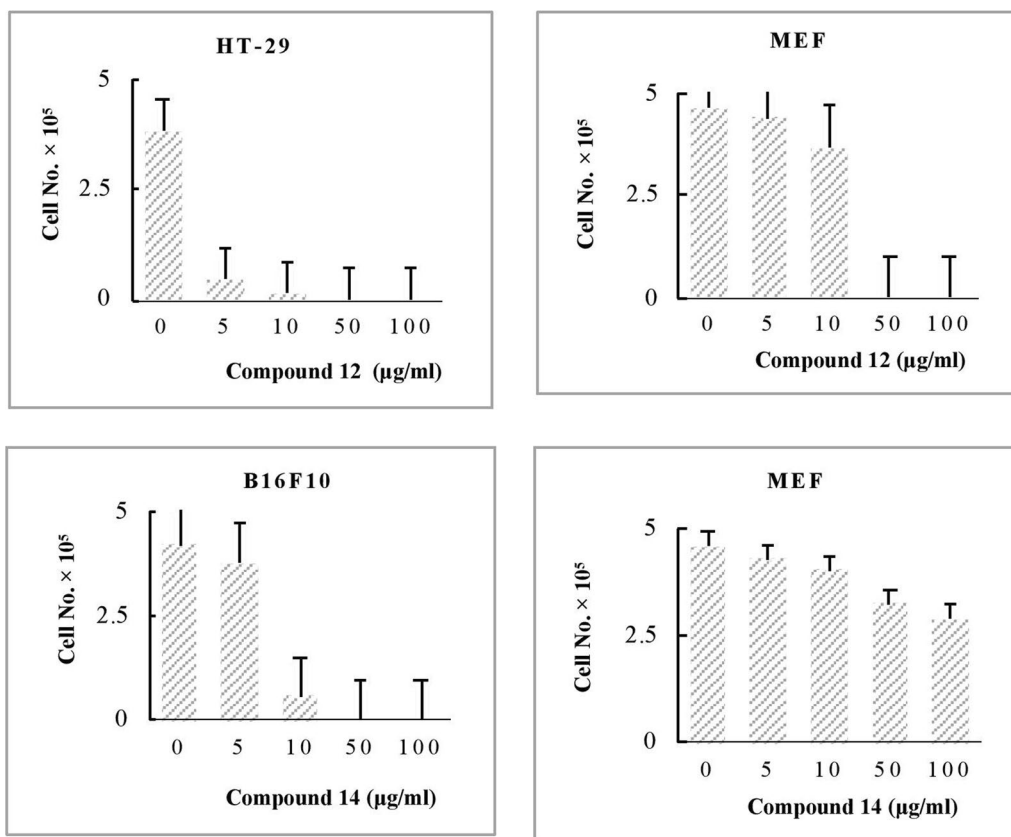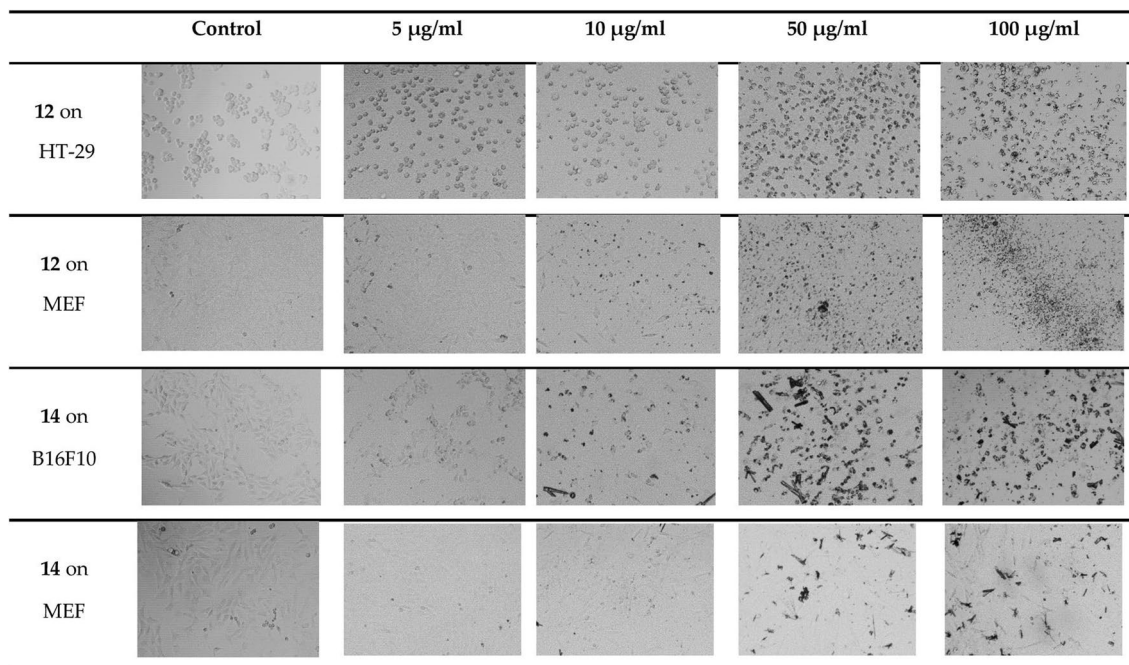The chemical compounds and solvents, procured from Sigma-Aldrich, were utilized without undergoing additional purification procedures. The 4-chlorophenyl isocyanide was synthesized using the methodology outlined by Weber and Gokel (1972) [27]. HPLC-grade methanol (MeOH) was acquired from Sigma-Aldrich and utilized for synthesis processes conducted under inert gas (N_2) conditions. ^{1}H-, ^{19}F-, and ^{13}C-NMR were recorded in CDCl$_3$ on 500 MHz Bruker AV III spectrometer. Chemical shifts are represented by the δ value (ppm), whereas coupling constants (*J*) are expressed in Hertz (Hz). The PerkinElmer 2400 analyzer was used to obtain the elementary analysis of C, H, and N. High-resolution mass spectra data (HRMS) were collected using the LTQ-Orbitrap XL (Thermo Fisher). FT-IR spectra were recorded on a Thermo Scientific Nicolet 1s5-Id3 Fourier transform infrared spectrophotometer. The progress of the reaction was monitored using aluminium-supported Thin Layer Chromatography (TLC) silica gel sheets (DC-Fertigfolien ALUGRAM® SIL G/UV254), and the spots were visualized using UV fluorescence. Moreover, silica gel from Sigma-Aldrich with a 60 Å pore size, 230–400 mesh, and 40–63 μm particle size under 5 psi compressed air was utilized for flash column chromatography. Solvents were evaporated using a Buchner Rotary Evaporator. Melting points were measured using Electrothermal Digital Mel-Temp 3.0 Melting Point apparatus. HPLC Waters Alliance e2695 equipped with a 2998 PDA detector (Waters Corporation, MA, USA) was used for the analysis of the synthesized compounds. RP C18 column (Restek Roc, 150×4.6 mm, 3 μm) was used, with a flow rate of 0.8 ml/minute. The DFT calculations were performed using the Gaussian09W software, employing the DFT/B3LYP/6-311G (d, p) methodology [28].

N-(4-chlorophenyl)−2-(2,3,4-trimethoxyphenyl) imidazo[1,2-a]pyridin-3-amine (9)

A mixture of 2-aminopyridine (282 mg, 3.0 mmol) and 2,3,4-trimethoxybenzaldehyde (589 mg, 3.0 mmol) containing Sc(OTf)$_3$ (74 mg, 0.15 mmol) and anhydrous Na$_2$SO$_4$ (300 mg) in MeOH: dichloromethane (1:1, 15 mL) was stirred under a nitrogen atmosphere for one hour at 50 °C. A solution of 4-chlorophenyl isocyanide (413 mg, 3.0 mmol) in MeOH (3 mL) was then added. After stirring at 60 °C for 3 h, the mixture was cooled to room temperature and stirred overnight. Water (10 mL) was added to the reaction mixture and extracted with ethyl acetate (3×15 mL). The combined organic layers were washed with water (20 mL), dried over Na$_2$SO$_4$,

filtered, and the solvent was evaporated under reduced pressure. The resultant residue was recrystallized twice with 95% ethanol to provide the pure compound **9** (429 mg, 34.8%) (Figure S1). MP: 219–219.8 °C; IR (cm^{-1}): 3221(N–H str.), 2946 (C–H str. in CH$_3$), 1598 (C=N str.), 1575 (C=C str.), 1489 (aromatic C=C str.), 1463 (C–H bending in CH$_3$), 1286 (C–O str.), 821 (C–Cl str.) (Figure S2); ^{1}H NMR (400 MHz, CDCl$_3$) δ ppm: 7.72 (dt, *J*=6.8, 1.2 Hz, 1H), 7.66 (dt, *J*=9.1, 1.1 Hz, 1H), 7.52 (d, *J*=8.7 Hz, 1H), 7.22 (ddd, *J*=9.1, 6.7, 1.3 Hz, 1H), 7.07 (d, *J*=8.8 Hz, 2 H), 6.81 (dt, *J*=8.8, 1.2 Hz, 2 H), 6.77 (s, 1H), 6.34 (d, *J*=8.9 Hz, 2 H), 3.93 (s, 3 H), 3.89 (s, 3 H), 3.72 (s, 3 H) (Figure S3); ^{13}C NMR (101 MHz, CDCl$_3$) δ ppm: 153.8, 150.9, 143.3, 142.2, 129.3, 125.5, 124.5, 124.2, 123.1, 120.7, 117.7, 115.5, 112.0, 108.6, 62.1, 61.2, 56.1. Anal. Calcd for C$_{22}$H$_{20}$ClN$_3$O$_3$ (409.87): C, 64.47; H, 4.92; N, 10.25%, found: C, 64.41; H, 8.64; N, 10.27%; HRMS *m/z* calcd for C$_{22}$H$_{19}$ClN$_3$O$_3$ ([M–H]$^-$) 408.1193, found 408.1114 (Figure S4).

2-(3-(Benzyloxy)−4-methoxyphenyl)-N-(4-chlorophenyl) imidazo[1,2-a]pyridin-3-amine (10)

A mixture of 2-aminopyridine (282 mg, 3.0 mmol) and 3-benzeloxy-4-methoxy-benzaldehyde (727 mg, 3.0 mmol) containing Sc(OTf)$_3$ (74 mg, 0.15 mmol) and anhydrous Na$_2$SO$_4$ (300 mg) in MeOH: dichloromethane (1:1, 15 ml) was stirred under a nitrogen atmosphere for one hour at 50 °C. The mixture was then subjected to the addition of a solution of 4-chlorophenyl isocyanide (413 mg, 3.0 mmol) in MeOH (3 mL), followed by the procedure described for **9**. The resultant residue was purified by flash chromatography (SiO$_2$, dichloromethane/ethyl acetate in 6:4 ratio) to yield the desired compound **10** (419 mg, 30.7%) (Figure S5). MP: 205.8–207.3 °C; IR (cm^{-1}): 3133 (N-H str.), 2931 (C–H str. in CH$_3$), 1585 (C=C str.), 1490 (aromatic C=C str.), 1467 (C–H bending in CH$_2$), 1257 (C–N str.), 1138 (C-O str.), 993 (C=C bending), 804 (C–Cl str.) (Figure S6); ^{1}H NMR (400 MHz, CDCl$_3$) δ ppm: 7.81 (dt, *J*=6.8, 1.2 Hz, 1H), 7.64 (d, *J*=9.0 Hz, 1H), 7.58 (td, *J*=8.3, 6.2, 2.0 Hz, 2 H), 7.43–7.31 (m, 4 H), 7.29 (tt, *J*=7.0, 6.3, 1.8 Hz, 1H), 7.24 (dd, *J*=9.0, 1.5 Hz, 1H), 7.15 (d, *J*=8.8 Hz, 2 H), 6.81 (t, *J*=7.2 Hz, 2 H), 6.54 (d, *J*=8.8 Hz, 2 H), 5.06 (s, 2 H), 4.30–4.16 (m, 1H), 3.86 (s, 3 H) (Figure S7); ^{13}C NMR (101 MHz, CDCl$_3$) δ ppm: 148.0, 136.9, 130.9, 129.8, 128.8, 128.4, 127.7, 127.3, 124.9, 122.7, 120.1, 114.7, 112.2, 111.7, 70.5, 68.2, 55.9, 38.7, 30.3, 28.9, 23.7, 23.0, 14.0, 11.0. (Figure S7); Anal. Calcd for C$_{27}$H$_{22}$ClN$_3$O$_2$ (455.94): C, 71,13; H, 4.86; N, 9.22%, found: C, 70.95; H, 4.88, N, 9.35%.

N-(4-chlorophenyl)−2-(1 H-indol-3-yl)imidazo[1,2-a]pyridin-3-amine (11)

A mixture of 2-aminopyridine (188 mg, 2.0 mmol) and 3-indolcarbaldehyde (290 mg, 2.0 mmol) containing $Sc(OTf)_3$ (49 mg, 0.1 mmol) and anhydrous Na_2SO_4 (200 mg) in MeOH: dichloromethane (1:1, 10 mL) was stirred under a nitrogen atmosphere for one hour at 50 °C. This was followed by the addition of a solution of 4-chlorophenyl isocyanide (275 mg, 2.0 mmol) in MeOH (2 mL). The mixture was then subjected to the procedure described for compound **9**. The resultant residue was purified by flash chromatography (SiO_2, dichloromethane/ethyl acetate in 1:1 ratio) to yield the desired compound **11** (224 mg, 31.4%) (Figure S8). MP: 269.2–270.8 °C; IR (cm^{-1}): 3357 (N–H str.), 3066 (C–H str. in $=$C–H), 1624 (C$=$N str.), 1597 (C$=$C str.), 1489 (aromatic C$=$C str.), 1330 (C–N str.), 815 (C–Cl str.) (Figure S9); ^{1}H NMR (400 MHz, CDCl$_3$) δ ppm: 8.47 (d, $J=7.5$ Hz, 1H), 8.25 (s, 1H), 7.82 (dt, $J=6.7$, 1.2 Hz, 1H), 7.69 (dt, $J=9.0$, 1.1 Hz, 1H), 7.47 (d, $J=2.7$ Hz, 1H), 7.40–7.35 (m, 1H), 7.24 (t, $J=1.5$ Hz, 1H), 7.22–7.21 (m, 1H), 7.20 (dt, $J=2.7$, 1.3 Hz, 1H), 7.16 (d, $J=8.8$ Hz, 2 H), 6.79 (td, $J=6.7$, 1.1 Hz, 1H), 6.56 (d, $J=8.9$ Hz, 2 H), 5.65 (s, 1H) (Figure S10); ^{13}C NMR (101 MHz, CDCl$_3$) δ ppm: 129.8, 114.6 (Figure S10); Anal. Calcd for $C_{21}H_{15}ClN_4$ (358.82): C, 70.29; H, 4.21; N, 15.61%, found: C, 70, 21; H, 4.17; N, 15.52%; HRMS m/z calcd for $C_{21}H_{16}ClN_4$ ([M+H]$^+$) 359.0985, found 359.1054 (Figure S11).

N-(4-chlorophenyl)−2-(2-nitrophenyl)imidazo[1,2-a]pyridin-3-amine (12)

A mixture of 2-aminopyridine (188 mg, 2.0 mmol) and 2-nitrobenzaldehyde (332 mg, 2.2 mmol) containing *p*-toluenesulfonic acid monohydrate (76 mg, 0.4 mmol) and anhydrous Na_2SO_4 (200 mg) in MeOH (10 mL) was stirred under a nitrogen atmosphere for one hour at 50 °C. This was followed by the addition of a solution of 4-chlorophenyl isocyanide (275 mg, 2.0 mmol) in MeOH (2 mL). The mixture was then subjected to the procedure described for **9** except for the reaction time that was 48 h. The resultant residue was purified by flash chromatography (SiO_2, dichloromethane / ethyl acetate in 7:3 ratio) to provide the compound **12** (293 mg, 40.0%) (Figure S12). MP: 173.3–175.4 °C; IR (cm^{-1}): 3140 (N-H str.), 1595 (C$=$C str.), 1521 (N-O str.), 1491 (aromatic C$=$C str.), 1347 (C-N str.), 819 (C–Cl str.) (Figure S13); ^{1}H NMR (400 MHz, CDCl$_3$) ppm: 7.86 (dd, $J=8.1$, 1.1 Hz, 1H), 7.80 (dt, $J=6.9$, 1.2 Hz, 1H), 7.73 (dd, $J=7.7$, 1.4 Hz, 1H), 7.66 (d, $J=9.1$ Hz, 1H), 7.59 (td, $J=7.6$, 1.3 Hz, 1H), 7.47 (td, $J=8.0$, 1.5 Hz, 1H), 7.36–7.27 (m, 1H), 7.1 (d, $J=8.9$ Hz, 2 H), 6.85

(t, $J=6.8$, 1.1 Hz, 1H), 6.42 (d, $J=8.8$ Hz, 2 H), 5.44 (s, 1H) (Figure S14); ^{13}C NMR (101 MHz, CDCl$_3$) δ ppm: 142.93, 142.86, 132.5, 132.1, 129.6, 128.9, 125.4, 124.4, 122.9, 118.3, 114.5, 112.8, 60.4, 21.1, 14.2, 1.0 (Figure S14); Anal. Calcd for $C_{19}H_{13}ClN_4O_2$ (364.78): C, 62.56; H, 3.59; N, 15.36%, found: C, 62.41; H, 3.57; N, 15.21%.

N-(4-chlorophenyl)−2-(furan-2-yl)imidazo[1,2-a]pyridin-3-amine (13)

A mixture of 2-aminopyridine (188 mg, 2.0 mmol) and 2-furaldehyde (193 mg, 2.0 mmol) containing $Sc(OTf)_3$ (49 mg, 0.1 mmol) and anhydrous Na_2SO_4 (200 mg) in MeOH (10 mL) was stirred under a nitrogen atmosphere for one hour at 50 °C. This was followed by the addition of a solution of 4-chlorophenyl isocyanide (303 mg, 2.2 mmol) in MeOH (2 mL). The mixture was then subjected to the procedure described for compound 9. The resultant residue was purified by flash chromatography (SiO_2, dichloromethane/ethyl acetate in 6:4 ratio) to furnish the title compound 13 (270 mg, 43.6%) (Figure S15). MP: 196.4–198.1 °C; IR (cm^{-1}): 3161 (N-H str.), 1599 (C$=$N str.), 1558 (C$=$C str.), 1490 (aromatic C$=$C str.), 1345 (C–N str.), 1260 (C–O str.), 820 (C–Cl str.) (Figure S16); ^{1}H NMR (400 MHz, CDCl$_3$) ppm: 7.83 (dt, $J=6.8$, 1.2 Hz, 1H), 7.62 (dt, $J=9.1$, 1.1 Hz, 1H), 7.46 (dd, $J=1.7$, 0.8 Hz, 1H), 7.26–7.20 (m, 1H), 7.15 (d, $J=8.8$ Hz, 2 H), 6.81 (td, $J=6.8$, 1.2 Hz, 1H), 6.74 (d, $J=3.1$ Hz, 1H), 6.51 (d, $J=8.8$ Hz, 2 H), 6.45 (dd, $J=3.4$, 1.8 Hz, 1H), 5.76 (s, 1H) (Figure S17); ^{13}C NMR (101 MHz, CDCl$_3$) δ ppm: 142.6, 129.6, 122.7, 115.1, 111.5 (Figure S17); Anal. Calcd for $C_{17}H_{12}ClN_3O$ (309.75): C, 65.92; H, 3.91; N, 13.57%. Found: C, 65.78; H, 3.94; N, 13.55%; HRMS m/z calcd for $C_{17}H_{11}ClN_3O$ ([M-H]$^-$) 308.0669, found 308.0591 (Figure S18).

N-(4-chlorophenyl)−2-(m-tolyl)imidazo[1,2-a]pyridin-3-amine (14)

A mixture of 2-aminopyridine (188 mg, 2.0 mmol) and *m*-tolualdehyde (240 mg, 2.0 mmol) containing $Sc(OTf)_3$ (49 mg, 0.1 mmol) and anhydrous Na_2SO_4 (200 mg) in MeOH (10 mL) was stirred under a nitrogen atmosphere for one hour at 50°C. This was followed by the addition of a solution of 4-chlorophenyl isocyanide (303 mg, 2.2 mmol) in MeOH (2 mL). The mixture was then subjected to the procedure described for 9. The resultant residue was purified by flash chromatography (SiO_2, dichloromethane/ethyl acetate in 8:2 ratio) to afford the desired compound 14 (342 mg, 51.2%) (Figure S19). MP: 183.4–184.3 °C; IR (cm^{-1}): 3203 (N–H str.), 2919 (C–H str. in CH$_3$), 1598 (C$=$N str.), 1569 (C$=$C str.), 1495 (aromatic C$=$C str.), 1344 (C–N str.), 818 (C–Cl str.) (Figure S20); ^{1}H NMR (500 MHz, CDCl$_3$) δ ppm: 7.84 (s, 1H), 7.80 (d, $J=6.9$ Hz, 1H), 7.69 (d, $J=7.8$ Hz, 1H), 7.63 (d, $J=9.1$

Hz, 1H), 7.25–7.22 (m, 1H), 7.21 (dd, J=3.6, 1.4 Hz, 1H), 7.15 (d, J=8.9 Hz, 2 H), 7.1 (d, J=7.6 Hz, 1H), 6.79 (td, J=6.8, 1.1 Hz, 1H), 6.51 (d, J=8.7 Hz, 2 H), 5.81 (s, 1H), 2.34 (s, 3 H) (Figure S21); ^{13}C NMR (126 MHz, CDCl$_3$) δ ppm: 143.3, 142.5, 138.3, 129.7, 128.9, 128.5, 127.7, 125.5, 124.7, 123.9, 122.6, 117.6, 117.4, 114.6, 112.5, 21.5 (Figure S21); Anal. Calcd for $C_{20}H_{16}ClN_3$ (333.81): C, 71.96; H, 4.83; N, 12.59%, found: C, 71.67; H, 85; N, 12.56%; HRMS m/z calcd for $C_{20}H_{15}ClN_3$ ([M–H]$^-$) 332.1033, found 332.0954 (Figure S22).

N-(4-chlorophenyl)−2-(2,3-dimethoxyphenyl)imidazo[1,2-a] pyridin-3-amine (15)

p-Toluenesulfonic acid monohydrate (76 mg, 0.4 mmol) was added to a mixture of 2-aminopyridine (188 mg, 2.0 mmol), 2,3-dimethoxybenzaldehyde (332 mg, 2.0 mmol) and anhydrous Na$_2$SO$_4$ (200 mg) in MeOH (10.0 mL). After stirring under a nitrogen atmosphere at 50 ℃ for one hour, a solution of 4-chlorophenyl isocyanide (303 mg, 2.0 mmol) in MeOH (2 mL) was added. The mixture was then subjected to the procedure described for compound 9. The residue was purified by flash column chromatography on silica gel in a 1:1 ratio of (dichloromethane /ethyl acetate in 1:1 ratio) to afford the title compound 15, which was further recrystallized from 95% of ethanol (372 mg, 49%) (Figure S23). MP: 220–221 ℃; IR (cm^{-1}): 2879 (C-H str. in CH$_3$), 1597 (C=N str.), 1580 (C=C str.), 1490 (aromatic C=C str.), 1348 (C-N str.), 1262 (C–O str.), 819 (C–Cl str.) (Figure S24); ^{1}H NMR (500 MHz, CDCl$_3$) ppm: 7.72–7.65 (m, 2 H), 7.46 (dd, J=8.0, 1.5 Hz, 1H), 7.23 (d, J=8.3 Hz, 1H), 7.19 (dd, J=8.0 Hz, 1H), 7.07 (d, J=8.8 Hz, 2 H), 6.95 (dd, J=8.1, 1.5 Hz, 1H), 6.91 (s, 1H), 6.82 (dd, J=7.3, 1H), 6.34 (d, J=8.9, 2 H), 3.92 (s, 3 H), 3.66 (s, 3 H) (Figure S25); ^{13}C NMR (126 MHz, CDCl$_3$) δ ppm: 152.6, 145.9, 142.7, 142.3, 129.2, 125.0, 124.6, 123.3, 123.0, 121.3, 117.8, 115.8, 112.1, 111.9, 61.6, 55.8, 31.6, 30.9, 22.7, 15.3, 14.1 (Figure S25); Anal. Calcd for $C_{21}H_{18}ClN_3O_2$ (379.84): C, 66.40; H, 4.78; N, 11.06%, found: C, 66.32; H, 4.79; N, 11.10%.

N-(4-chlorophenyl)−2-(naphthalen-2-yl)imidazo[1,2-a] pyridin-3-amine (16)

A mixture of 2-aminopyridine (188 mg, 2.0 mmol) and 2-naphthaldehyde (312 mg, 2.0 mmol) containing *p*-toluenesulfonic acid monohydrate (76 mg, 0.4 mmol) and sodium sulphate (200 mg) in MeOH (10 mL) was stirred under a nitrogen atmosphere for one hour at 50 ℃. Then, a solution of 4-chlorophenyl isocyanide (303 mg, 2.2 mmol) in MeOH (2 mL) was added, and the mixture was subjected to the procedure described for 9. Purification by flash column chromatography (SiO$_2$, dichloromethane/ethyl acetate in 6:4 ratio), followed by recrystallization from 95% ethanol yielded 16 as white crystals (354 mg, 47.9%) (Figure S26). MP: 225.7–226.7 ℃; IR (cm^{-1}): 3198 (N-H str.), 3073 (C-H str. in =C-H), 1600 (C=N str.), 1569 (C=C str.), 1491 (aromatic C=C str.), 1344 (C–N str.), 815 (C–Cl str.) (Figure S27); ^{1}H NMR (500 MHz, CDCl$_3$) δ ppm: 8.47 (s, 1H), 8.08 (dd, J=8.6, 1.6 Hz, 1H), 7.87–7.74 (m, 4 H), 7.66 (d, J=9.0 Hz, 1H), 7.46 (dt, J=9.4, 3.1 Hz, 2 H), 7.26–7.21 (m, 1H), 7.18 (d, J=8.8 Hz, 2 H), 6.79 (t, J=6.8, 1.1 Hz, 1H), 6.57 (d, J=8.7 Hz, 2 H), 5.71 (s, 1H) (Figure S28); ^{13}C NMR (126 MHz, CDCl$_3$) δ ppm: 143.3, 142.9, 133.4, 133.0, 129.8, 128.5, 128.2, 127.6, 126.2, 125.4, 124.78, 124.65, 122.6, 117.86, 117.69, 114.7, 112.5 (Figure S28); Anal. Calcd for $C_{23}H_{16}ClN_3$ (369.85): C, 74.69; H, 4.36; N, 11.36% found: C, 74.38; H, 4.32; N, 11.34%.

N-(4-chlorophenyl)−2-(thiophen-3-yl)imidazo[1,2-a] pyridin-3-amine (17)

A mixture of 2-aminopyridine (188 mg, 2.0 mmol) and 3-thiophenecarboxaldehyde (230 mg, 2.0 mmol) containing *p*-toluenesulfonic acid monohydrate (76 mg, 0.4 mmol) and sodium sulphate (200 mg) in MeOH (10 mL) was stirred under a nitrogen atmosphere for one hour at 50 ℃. Then, a solution of 4-chlorophenyl isocyanide (303 mg, 2.2 mmol) in MeOH (2 mL) was added, and the mixture was subjected to the procedure described for **9**. The residue was recrystallized with 95% ethanol twice, yielded compound 17 as hairy crystals (214 mg, 32.8%) (Figure S29). MP: 245.8–246.9 ℃; IR (cm^{-1}): 3209 (N-H str.), 1631 (C=N str.), 1595 (C=C str.), 1492 (aromatic C=C str.), 1345 (C–N str.), 1093 (C=S str.), 816 (C–Cl str.) (Figure S30); ^{1}H NMR (500 MHz, CDCl$_3$) δ ppm: 7.83 (d?, J=6.9 Hz, 1H), 7.76 (dd, J=3.0, 1.1 Hz, 1H), 7.67–7.57 (m, 2 H), 7.33 (dd, J=5.2, 3.0 Hz, 1H), 7.24 (ddd, J=9.1, 6.8, 1.3 Hz, 1H), 7.16 (d, J=8.8 Hz, 2 H), 6.80 (dd, J=6.8, 1.1 Hz, 1H), 6.53 (d, J=8.9 Hz, 2 H), 5.58 (s, 1H) (Figure S31); ^{13}C NMR (126 MHz, CDCl$_3$) δ ppm: 143.3, 142.9, 136.8, 134.4, 129.8, 126.4, 125.91, 125.26, 124.8, 122.69, 122.44, 117.6, 116.8, 114.5, 112.4 (Figure S31); Anal. Calcd for $C_{17}H_{12}ClN_3S$ (325.81): C, 62.67; H, 3.71; N, 12.90%, found: C, 62.26; H, 3.72; N, 12.92%.

N-(4-chlorophenyl)−2-(2,4-difluorophenyl)imidazo[1,2-a] pyridin-3-amine (18)

A mixture of 2-aminopyridine (188 mg, 2.0 mmol), and 2,4-difluorobenzaldehyde (284 mg, 2.0 mmol) containing *p*-toluenesulfonic acid monohydrate (76 mg, 0.4 mmol) in MeOH (10 mL) was stirred under a nitrogen atmosphere for one hour at 50 ℃. This was followed by the addition of a solution of 4-chlorophenyl isocyanide (303 mg, 2.2 mmol) in MeOH (2 mL). The mixture was then subjected to the procedure described for **9.** The resultant residue was purified by flash chromatography (SiO$_2$, dichloromethane/ethyl acetate in 8:2 ratio) to yield the

Al-Qadi *et al. BMC Chemistry*   (2025) 19:48

Page 13 of 15

desired compound **18** (259 mg, 36.6%) (Figure S32). MP: 154.8–156.9 °C; IR (cm^{-1}): 3160 (N-H str.), 3080 (C–H str. in = C–H), 1597 (C=N str.), 1574 (C=C str.), 1491 (aromatic C=C str.), 1266 (C-N str.), 1141 (C-F str.); 970 (C=C bending), 818 (C-Cl str.) (Figure S33); ^{1}H NMR (400 MHz, CDCl$_3$) δ ppm: 7.83 (d, *J* = 8.5 Hz, 1H), 7.8 (d, *J* = 8.5 Hz, 1H), 7.66 (d, *J* = 9.1 Hz, 1H), 7.27 (ddd, *J* = 9.0, 6.7, 1.2 Hz, 1H), 7.11 (d, *J* = 8.8 Hz, 2 H), 6.96 (td, *J* = 8.2, 2.7 Hz, 1H), 6.91–6.84 (m, 1H), 6.83 (dd, *J* = 6.7, 2.4 Hz, 1H), 6.41 (d, *J* = 8.9 Hz, 2 H), 5.76 (d, *J* = 2.7 Hz, 1H) (Figure S34); ^{13}C NMR (101 MHz, CDCl3) δ ppm: 164.21, 164.08, 161.72, 161.60, 161.17, 161.05, 158.69, 158.57, 143.18, 143.0, 134.0, 132.28, 132.23, 132.19, 132.13, 129.5, 125.2, 124.7, 123.0, 119.7, 118.0, 114.8, 112.51, 112.11, 112.08, 111.90, 111.87, 104.46, 104.20, 103.9 (Figure S34); ^{19}F NMR (377 MHz, CDCl3) δ ppm: − 109.16, − 110.27 (Figure S35); Anal. Calcd for C$_{19}$H$_{12}$ClF$_2$N$_2$ (355.77): C, 64.14; H, 3.40; N, 11.81%, found: C, 64.11; H, 3.41; N, 11.83%.

N-(4-chlorophenyl)−2-(4-(trifluoromethyl)phenyl) imidazo[1,2-a]pyridin-3-amine (19)

A mixture of 2-aminopyridine (188 mg, 2.0 mmol), 4-tri-fluoromethyl-benzaldehyde (348 mg, 2.0 mmol), *p*-tol-uenesulfonic acid monohydrate (76 mg, 0.4 mmol) and Na$_2$SO$_4$ (200 mg) in MeOH (10 mL) was stirred under a nitrogen atmosphere for one hour at 50 °C. This was followed by the addition of 4-chlorophenyl isocyanide (280 mg, 2.0 mmol). The mixture was then subjected to the procedure described for **9**. The residue was purified by flash column chromatography (SiO$_2$, dichloromethane/ ethyl acetate in 7:3 ratio) to yield the desired compound **19** as pale-yellow solid (240 mg, 30.9%) (Figure S36). MP: 197.5–199 °C; IR (cm^{-1}): 3147 (N-H str.), 3069 (C–H str. in = C–H), 1621 (C=N str.), 1599 (C=C str.), 1490 (aromatic C=C str.), 1323 (C–N str.), 1120 (C–F str.), 825 (C–Cl str.) (Figure S37); ^{1}H NMR (400 MHz, CDCl$_3$) ppm: 8.11 (d, *J* = 8.1 Hz, 2 H), 7.83 (dt, *J* = 6.8, 1.2 Hz, 1H), 7.66 (dt, *J* = 9.1, 1.1 Hz, 1H), 7.62 (d, *J* = 8.7 Hz, 2 H), 7.29 (dd, *J* = 9.1, 6.7, 1.3 Hz, 1H), 7.18 (d, *J* = 8.8 Hz, 2 H), 6.83 (td, *J* = 7.9, 6.8, 1.1 Hz, 1H), 6.54 (d, *J* = 8.8 Hz, 2 H), 5.69 (s, 1H) (Figure S38); ^{13}C NMR (101 MHz, CDCl$_3$) δ ppm: 142.9, 136.6, 129.92, 129.55, 129.23, 127.1, 125.84, 125.59, 125.55, 125.15, 122.7, 118.3, 118.0, 114.6, 112.9 (Figure S38); ^{19}F NMR (377 MHz, CDCl3) δ ppm: −62.58 (Figure S39); Anal. Calcd for C$_{20}$H$_{13}$ClF$_3$N$_3$ (387.07): C, 61.95; H, 3.38; N, 10.84%, found: C, 61.82; H, 3.42; N, 10.81%.

XRD-Analysis

Using Crystal Explorer 3.1, HSA computations were performed [29]. The XRD-crystallographic data for the desired ligand was acquired at a temperature of 296 °K using the CrysalisPro program [30]. This was accomplished with Mo radiation (wavelength = 0.71073) and a Gemini kappa-geometry diffractometer, especially a Rigaku XtaLAB P200K fitted with an Atlas CCD detector. SHELXT [31] was used to make the structural determination. Table S2 displays the parameters and crystallographic data used to refine the structure of compound **15**.

Biological activity

Anticancer activity

The synthesized compounds were assessed for their cytotoxic effects on three different cancer cell lines: the MCF-7 human breast cancer cell line (ATCC number: HTB-22), the HT-29 human colorectal adenocarcinoma cell line [HTB-38; American Type Culture Collection (ATCC), Manassas, VA, USA], and the B16F10 murine melanoma cancer cell line [CRL-6475; American Type Culture Collection (ATCC), Manassas, VA, USA], as well as the normal cell line mouse Embryonic Fibroblast-1 cell line (MEF-1; ATCC CRL-2214). The cell line was cultivated in high-glucose Dulbecco's Modified Eagle Medium (DMEM) that is supplemented with L-glutamine, phenol red (Fuji Film Wako, Osaka, Japan), 10% fetal bovine serum (FBS; G.E. Healthcare, Chicago, IL, USA), and 1% penicillin/streptomycin (P/S) (Nacalai Tesque, Kyoto, Japan). Exponentially growing cells (1×10^5 cells/well) were seeded in a 24-well plate with sterile-filtered DMEM medium at 37 °C under 5% CO$_2$ and incubated overnight. The cells were then treated with different concentrations of test compounds (5, 10, 50, and 100 μg/mL) and incubated for 24 h in a humidified atmosphere. After 24 h of incubation, viable cells were counted in each well using the Trypan blue exclusion test. All compounds were initially dissolved in DMSO, and the final concentration of DMSO was less than 1% in all of the considered concentrations of the applied compounds. The IC$_{50}$ values from at least two independent experiments were compared with the control and expressed as the mean ± SD. The analysis of two groups was performed using the student t-test, and P-values < 0.05 were statistically significant.

Abbreviations

IR	Infrared
FTIR	Fourier-transform infrared spectroscopy
HPLC	High-performance liquid chromatography
HRMS	High-resolution mass spectrometry
^{1}H NMR	Proton nuclear magnetic resonance
^{13}C NMR	Carbon nuclear magnetic resonance
DFT	Density functional theory
μM	Micromolar
°C	Degree centigrade
h	Hour
g	Gram
mg	Milligram
mL	Millilitre
μL	Microliter
DMSO	Dimethylsulfoxide

Al-Qadi *et al. BMC Chemistry*   (2025) 19:48

Page 14 of 15

XDR/HSA   X-ray Diffraction/Human Serum Albumin

Supplementary Information

The online version contains supplementary material available at https://doi.org/10.1186/s13065-025-01412-6.

> Supplementary Material 1.

Author contributions

Conceptualization, N.A.M. and S.R.; methodology, I.A.; software, I.W.; validation, I.Q., R.H., M.H. and N.A.M.; formal analysis, N.A.M.; investigation, I.Q., R. H. and N.A.M.; resources, M.H.; writing—original draft preparation, I.Q., N. A.M., I.W.; writing—review and editing, N.A.M.,Y.S., N.A.H., M.H, and S.R; visualization, S.R; supervision, N.A.M. M.H. and S.R.; project administration, N.A.M and S.R.; funding acquisition, N.A.M. and S.R. All authors have read and agreed to the published version of the manuscript.

Availability of data and materials

The data underlying this study are available in the published article and its online supplementary material. Supporting information is freely accessible online and includes the supplementary crystallographic data for this paper (CCDC No. 2401478). These data can be obtained free of charge via https://www.ccdc.cam.ac.uk/structures/Search? access=referee&ccdc=2401478&Author=Saki+Raheem, by emailing data_request@ccdc.cam.ac.uk, or by contacting The Cambridge Crystallographic Data Centre, 12 Union Road, Cambridge CB2 1EZ, UK; fax: +44-1223-336033.

Declarations

Ethics approval and consent to participate
Not applicable.

Consent for publication
Not applicable.

Competing interests
The authors declare no competing interests.

References

1. Kim O, Jeong Y, Lee H, Hong SS, Hong S. Design and synthesis of imidazopyridine analogues as inhibitors of phosphoinositide 3-kinase signaling and angiogenesis. J Med Chem. 2011;54(7):2455–66. https://doi.org/10.1021/jm101582z.
2. Kamal A, Kumar GB, Nayak VL, Reddy VS, Shaik AB, Reddy MK. Design, synthesis and biological evaluation of imidazopyridine/imidazopyrimidine-benzimidazole conjugates as potential anticancer agents. MedChemComm. 2015;6(4):606–12. https://doi.org/10.1039/C4MD00400K.
3. Muniyan S, Chou YW, Ingersoll MA, Devine A, Morris M, Odero-Marah VA, Khan SA, Chaney WG, Bu XR, Lin MF. Antiproliferative activity of novel imidazopyridine derivatives on castration-resistant human prostate cancer cells. Cancer Lett. 2014;353(1):59–67. https://doi.org/10.1016/j.canlet.2014.07.002.
4. Khatun S, Singh A, Bader GN, Sofi FA. Imidazopyridine, a promising scaffold with potential medicinal applications and structural activity relationship (SAR): recent advances. J Biomol Struct Dynamics. 2022;40(24):14279–302. https://doi.org/10.1080/07391102.2021.1997818.
5. Aliwaini S, Awadallah AM, Morjan RY, Ghunaim M, Alqaddi H, Abuhamad AY, Awadallah EA, Abughefra YM. Novel imidazo [1, 2a] pyridine inhibits AKT/mTOR pathway and induces cell cycle arrest and apoptosis in melanoma and cervical cancer cells. Oncol Lett. 2019;18(1):830–7. https://doi.org/10.3892/ol.2019.10341.
6. Sonawane RS, Patil KD, Patil AV. Design, synthesis and pharmacological evaluation of novel imidazopyridine analogues as proton pump antagonist. Asian J Chem. 2020;32(4):776–82. https://doi.org/10.14233/ajchem.2020.22433.
7. Fan YH, Li W, Liu DD, Bai MX, Song HR, Xu YN, Lee S, Zhou ZP, Wang J, Ding HW. Design, synthesis, and biological evaluation of novel 3-substituted imidazo [1, 2-a] pyridine and quinazolin-4 (3H)-one derivatives as PI3Kα inhibitors. Eur J Med Chem. 2017;139:95–106. https://doi.org/10.1016/j.ejmech.2017.07.074.
8. Baviskar AT, Madaan C, Preet R, Mohapatra P, Jain V, Agarwal A, Guchhait SK, Kundu CN, Banerjee UC, Bharatam PV. N-fused imidazoles as novel anticancer agents that inhibit catalytic activity of topoisomerase IIα and induce apoptosis in G1/S phase. J Med Chem. 2011;54(14):5013–30. https://doi.org/10.1021/jm200235u.
9. Yadav UP, Ansari AJ, Arora S, Joshi G, Singh T, Kaur H, Dogra N, Kumar R, Kumar S, Sawant DM, Singh S. Design, synthesis and anticancer activity of 2-arylimidazo [1, 2-a] pyridinyl-3-amines. Bioorg Chem. 2022;118:105464. https://doi.org/10.1016/j.bioorg.2021.105464.
10. Garamvölgyi R, Dobos J, Sipos A, Boros S, Illyés E, Baska F, et al. Design and synthesis of new imidazo[1,2-a]pyridine and imidazo[1,2-a]pyrazine derivatives with antiproliferative activity against melanoma cells. Eur J Med Chem. 2016;108:623–43. https://doi.org/10.1016/j.ejmech.2015.12.001.
11. Gueiffier A, Mavel S, Lhassani M, Elhakmaoui A, Snoeck R, Andrei G, et al. Synthesis of Imidazo[1,2- a]pyridines as antiviral agents. J Med Chem. 1998;41(25):5108–12. https://doi.org/10.1021/jm981051y.
12. Ismail MA, Brun R, Wenzler T, Tanious FA, Wilson WD, Boykin DW. Novel Dicationic Imidazo[1,2- a]pyridines and 5,6,7,8-Tetrahydro-imidazo[1,2- α] pyridines as Antiprotozoal agents. J Med Chem. 2004;47(14):3658–64. https://doi.org/10.1021/jm0400092.
13. Dahan-Farkas N, Langley C, Rousseau AL, Yadav DB, Davids H, de Koning CB. 6-Substituted imidazo[1,2-a]pyridines: synthesis and biological activity against colon cancer cell lines HT-29 and Caco-2. Eur J Med Chem. 2011;46(9):4573–83. https://doi.org/10.1016/j.ejmech.2011.07.036.
14. Al-Tel TH, Al-Qawasmeh RA, Zaarour R. Design, synthesis and in vitro antimicrobial evaluation of novel Imidazo[1,2- α]pyridine and imidazo[2,1-b] [1,3]benzothiazole motifs. Eur J Med Chem. 2011;46(5):1874–81. https://doi.org/10.1016/j.ejmech.2011.02.051.
15. Bagdi AK, Santra S, Monir K, Hajra A. Synthesis of imidazo[1,2-a]pyridines: a decade update. Chem Commun. 2015;51(9):1555–75. https://doi.org/10.1039/C4CC08495K.
16. Groebke K, Weber L, Mehlin F. Synthesis of Imidazo[1,2-a] annulated pyridines, Pyrazines and Pyrimidines by a Novel three-component condensation. Synlett. 1998;1998(06):661–3. https://doi.org/10.3762/bjoc.19.53.
17. Blackburn C, Guan B, Fleming P, Shiosaki K, Tsai S. Parallel synthesis of 3-aminoimidazo[1,2-a]pyridines and pyrazines by a new three-component condensation. Tetrahedron Lett. 1998;39(22):3635–8. https://doi.org/10.1016/S0040-4039(98)00653-4.
18. Boltjes A, Dömling A. The Groebke-Blackburn-Bienayme reaction. Eur J Org Chem. 2019;201942:7007–49. https://doi.org/10.1002/ejoc.201901124.
19. Nisar S, Masoodi T, Prabhu KS, Kuttikrishnan S, Zarif L, Khatoon S, Ali S, Uddin S, Akil AAS, Singh M, Macha MA. Natural products as chemo-radiation therapy sensitizers in cancers. Biomed Pharmacother. 2022;154:113610. https://doi.org/10.1016/j.biopha.2022.113610.
20. Kaur R, Bhardwaj A, Gupta S. Cancer treatment therapies: traditional to modern approaches to combat cancers. Mol Biol Rep. 2023;50(11):9663–76. https://doi.org/10.1007/s11033-023-08809-3.
21. Yang L, Shi P, Zhao G, Xu J, Peng W, Zhang J, Zhang G, Wang X, Dong Z, Chen F, Cui H. Targeting cancer stem cell pathways for cancer therapy. Signal Transduct Target Therapy. 2020;5(1):8. https://doi.org/10.1038/s41392-020-0110-5.
22. Cesur-Ergün B, Demir-Dora D. Gene therapy in cancer. J Gene Med. 2023;25(11):e3550. https://doi.org/10.1002/jgm.3550.
23. Gavas S, Quazi S, Karpiński TM. Nanoparticles for cancer therapy: current progress and challenges. Nanoscale Res Lett. 2021;16(1):173. https://doi.org/10.1186/s11671-021-03628-6.

Al-Qadi *et al. BMC Chemistry*   *(2025) 19:48*

Page 15 of 15

24. Sun L, Liu H, Ye Y, Lei Y, Islam R, Tan S, Tong R, Miao YB, Cai L. Smart nano-particles for cancer therapy. Signal Transduct Target Ther. 2023;8(1):418. https://doi.org/10.1038/s41392-023-01642-x.
25. Chen H, Han Z, Luo Q, Wang Y, Li Q, Zhou L, Zuo H. Radiotherapy modu-lates tumor cell fate decisions: a review. Radiat Oncol. 2022;17(1):196. https://doi.org/10.1186/s13014-022-02171-7.
26. Galluzzi L, Aryankalayil MJ, Coleman CN, Formenti SC. Emerging evidence for adapting radiotherapy to immunotherapy. Nat Reviews Clin Oncol. 2023;20(8):543–57. https://doi.org/10.1038/s41571-023-00782-x.
27. Weber WP, Gokel GW. An improved procedure for the Hofmann carby-lamine synthesis of isonitriles. Tetrahedron Lett. 1972;13(17):1637–40. https://doi.org/10.1016/S0040-4039(01)84707-9.
28. Ali M, Mansha A, Asim S, Zahid M, Usman M, Ali N. DFT study for the spectroscopic and structural analysis of p-dimethylaminoazobenzene. J Spectrosc. 2018;2018(1):9365153. https://doi.org/10.1155/2018/9365153.
29. McKinnon JJ, Spackman MA, Mitchell AS. Novel tools for visualizing and exploring intermolecular interactions in molecular crystals. Acta Crystal-logr B. 2004;60(6):627–68. https://doi.org/10.1107/S0108768104020300.
30. Agilent, Technologies. CrysAlisPro, Version 1.171.36.20. Data collection and processing software for agilent X-ray diffractometers. Agilent Tech-nologies. 2013. https://www.agilent.com/cs/library/usermanuals/Public/CrysAlis_Pro_User_Manual.pdf. Accessed 18 Jun 2024.
31. Sheldrick GM. SHELXT–Integrated space-group and crystal-structure determination. Acta Crystallogr Foud Adv. 2015;71(1):3–8. https://doi.org/10.1107/S2053273314026370.

Publisher's note
Springer Nature remains neutral with regard to jurisdictional claims in pub-lished maps and institutional affiliations.